NACA TN 3332

NATIONAL ADVISORY COMMITTEE FOR AERONAUTICS

TECHNICAL NOTE 3332

BURNING TIMES OF MAGNESIUM RIBBONS IN VARIOUS ATMOSPHERES

By Kenneth P. Coffin

Lewis Flight Propulsion Laboratory
Cleveland, Ohio

Washington

December 1954

THIS DOCUMENT ON LOAN FROM THE FILES OF
NATIONAL ADVISORY COMMITTEE FOR AERONAUTICS
LANGLEY AERONAUTICAL LABORATORY
LANGLEY FIELD, HAMPTON, VIRGINIA
RETURN TO THE ABOVE ADDRESS.

REQUESTS FOR PUBLICATIONS SHOULD BE ADDRESSED AS FOLLOWS:
NATIONAL ADVISORY COMMITTEE FOR AERONAUTICS
1512 H STREET, N. W.
WASHINGTON 25, D. C.

NATIONAL ADVISORY COMMITTEE FOR AERONAUTICS

TECHNICAL NOTE 3332

BURNING TIMES OF MAGNESIUM RIBBONS IN VARIOUS ATMOSPHERES

By Kenneth P. Coffin

3277

T-OO

SUMMARY

Some details of the physical mechanism of the combustion of magnesium ribbon were investigated, and burning times for magnesium ribbons were determined with various mixtures of oxygen in argon, nitrogen, helium, and argon - water vapor. Evidence from this investigation indicates that a gas-phase rather than a surface reaction occurs, which bears some analogy to the combustion of liquid-fuel drops. The experimental burning times are compared with those calculated by using a vapor-phase heat- and mass-transfer mechanism. The infinitesimally thin flame front concept successfully applied to fuel drops was abandoned in favor of a high-temperature reaction zone of finite thickness. Agreement between experimental and calculated values for burning time in terms of oxygen concentration for the argon- and nitrogen-inerted systems was quite satisfactory on a relative basis; actual numerical values agreed within a factor of 2 to 3. Agreement was less satisfactory for low-density helium-inerted atmospheres, although the changes observed experimentally were in the direction indicated by the calculation.

For the geometry employed, observed burning times (approximately proportional to reciprocal average burning rates) decreased by a factor of approximately 10 with increasing oxygen concentration over the range 17 to 100 percent by volume. The times were slightly longer with argon mixtures than with nitrogen mixtures and appreciably shorter with helium than with argon or nitrogen. Burning times decreased by as much as one third with increasing moisture content; the greatest changes occurred for small amounts of water vapor and for long burning times.

INTRODUCTION

In spite of the expanded efforts on combustion research in recent years, the burning of metallic solids has not received much attention. While solid carbon has been the subject of extensive investigations, which clearly indicate the significance of surface reaction in the utilization of nonvolatile carbon, there is relatively little information available on the detailed mechanism of the combustion of metals. A

possible reason for this lack of information is that previous investigators may have generally assumed that the burning of metal solids resembles that of liquid hydrocarbons.

Work on the carbon problem has ranged from the isolation of the surface reactions (refs. 1 to 3) and the burning of carbon rods and single carbon spheres in air streams (refs. 4 to 6) to complex studies of fuel beds (ref. 7), coal-gasification projects (ref. 8), and the powdered-coal gas turbine (ref. 9). The utilization of solid explosives, primarily as ammunition (ref. 10), is another aspect of solid combustion which has received much attention. A project has also been conducted in the attainment of high temperature by burning metals (ref. 11).

3277

In a somewhat different vein, dust explosions, first of coal, flour, and sugar, and more recently of metallic dusts in powder metallurgy, have attracted attention from the point of view of safety; ignition energies, explosive limits, pressure rises, and rates of pressure rise have been studied (ref. 12). Closer to the subject is work on the propagation of flame through dust clouds: the experimental flame speed of aluminum powder dust together with the effects of concentration and particle size (ref. 13), spectral studies of metal dust flames (ref. 14), and work with metal dusts in Bunsen burners including the determination of flame temperatures (refs. 15 and 16).

Of much general interest, but little direct significance, is the considerable volume of work on the high-temperature slow oxidation of metals; that is, studies of the growth of oxide films at temperatures below those at which ignition occurs. These investigations (refs. 17 and 18), covering a wide range of metals, definitely involve metallic surface phenomena. Of more specific interest are studies of the burning of single liquid fuel drops (refs. 19 to 21), and of liquid fuel from burners of various geometries (ref. 22). In such cases, where vapor processes are known to occur, successful techniques for the treatment of single diffusion flames have been developed. A summary of the influence of inert gases on homogeneous gaseous flame phenomena has been prepared (ref. 23). (The inert gases used in the experiments described in this report are included in ref. 23.)

The purpose of this investigation was to study the gross physical mechanism of the combustion of magnesium metal in order to learn whether a vapor-phase or surface reaction is involved; further, to examine the effect of the composition of the oxidizing atmosphere, both as a matter of general interest and in the hope that such studies might be informative as to the details of the physical and/or chemical processes involved. In particular, magnesium ribbon was burned in 17- to 100-percent oxygen mixtures with argon, nitrogen, helium, and argon - water vapor as diluents. Data are presented in terms of burning times for a strip of ribbon about 4.6 centimeters long; such data bear an approximately inverse relation to average burning rates. The experimental data are

compared with average burning times calculated from hypotheses involving diffusion and heat-transfer relations; the effects of moisture are less satisfactorily explained. The occurrence of a vapor-phase combustion process is strongly indicated on the basis of (1) the experimental observations and (2) the comparison between experimental and calculated burning times.

3277 CO-1 back

APPARATUS

Box. - All experiments were carried out in a cubical box with an inner dimension of 7 inches, constructed of 1/2-inch transparent plastic (fig. 1). A rectangular access port in the top was covered by a metal plate with a sheet of heavy gasket material attached; the cover served as an adequate seal under vacuum conditions and as a vent against pressures above atmospheric. A rubber stopper in the bottom supported two electrodes and a tube for evacuating and filling the box. The tube was connected to the gas source, and through a filter to a pressure gage and the laboratory vacuum system. The magnesium ribbon was supported by a metal bracket with a gap of about 4.6 centimeters and held in place by small metal weights.

Ignition. - The electrodes supported a heater in the shape of a squared "U" about 1.5 centimeters across and formed from about 8 centimeters of number 16 Nichrome wire. To produce ignition, a thread, consisting of one third of a 7.5-centimeter magnesium ribbon, was wrapped tightly about the cross bar of the heater and placed just under the ribbon; 4 volts across the heater fired the thread, and the thread in turn ignited the ribbon.

Magnesium ribbon. - The magnesium ribbon measured 0.015 by 0.31 centimeter and weighed 0.0074 gram per centimeter (about 10 percent less than weight calculated from dimensions). No special precautions were taken to remove oxide film or prevent oxidation, but the ribbons were kept in closed containers and retained their luster.

Gases. - Mixtures of 17.6, 21.5, 24.1, 34.2, and 43.7 volume percent oxygen in argon were obtained commercially and the analyses checked. The 18.2, 32.0, and 70.6 percent oxygen in argon and the 18.0 and 53.0 percent oxygen in helium were mixed in the laboratory from cylinders of the individual gases in a 35-liter tank to a total pressure of 5 atmospheres. Compressed air and mixtures of 34.9, 44.5, and 70.0 percent oxygen in nitrogen were also obtained commercially.

Water vapor. - Moisture was added to the 21.5 and 43.7 percent oxygen in argon mixtures by flowing the gas mixture over water in a simple train; the amount of water taken up was varied by adjusting the ratio of gas flowing through the train and through a dry bypass.

The concentration of water in the mixture was determined in terms of the dew-point temperature; with adequate conditioning of the instrument, readings obtained before and after runs of several hours checked to within about 5 percent of the amount of water present.

Cameras. - Motion pictures were taken at about 16 frames per second with spring-driven cameras calibrated for speed and constancy of speed. Detailed still pictures were obtained with a view camera.

3277

PROCEDURE

Obtaining Data

The procedure used for obtaining data was as follows: The thread and the ribbon were placed in position. The box was twice evacuated to a pressure of 25 to 40 millimeters and filled with the selected mixture. In addition, for mixtures containing moisture, the box was purged for 8 to 10 minutes (three to four times the period required to fill the box at the flow rates used in the train). The only effects of procedure were found for mixtures containing water vapor. External electrical and photographic adjustments were made while the box was being filled. With all preparations completed, the heater current was turned on and then shut off when the thread ignited. The motion-picture camera was started at the first glow of the Nichrome; the still camera was snapped manually.

Reducing Data

In the reduction of data, all quantitative results were derived from the motion pictures. Selected and numbered frames are shown in figure 2 for a test with a burning time of about 3 seconds.

Burning time. - The time elapsed between the start and the finish of the burning of the magnesium ribbon spanning the 4.6-centimeter gap in the metal bracket is defined as the burning time. No corrections were made on the burning-time measurements for the action of the igniter or for the quenching effect of the metal bracket (burning approached the bracket somewhat more closely for shorter burning times). The start was taken as the first frame showing a flame which within several frames was observed to be spreading (extending horizontally). For example, in figure 2 no spreading occurs between frames -10, -5, and 0, but by frame 5 spreading is underway; therefore, 0 is taken as the start (in practice, with a viewer, this procedure is capable of finer gradations). Frame 30 shows fully developed combustion. By frame 37 the flame is starting to subside. An appreciably decreased luminous area is shown in frame 45, and frame 50 indicates the final stages of vigorous burning. Frame 53 shows a luminosity which thereafter changes relatively slowly with time (it persists considerably beyond frame 59). Therefore, frame 53, as an

intermediate condition between vigorous burning and residual luminosity, is taken as the end. On the whole, the reproducibility of this measuring procedure is apparently quite adequate (the spread of the data is shown in fig. 5); the data are of such a nature that a systematic error of a few frames, either as a constant or as a percentage error, will have little effect in the final comparisons.

Apparent flame diameter. - The distance from the bottom of the luminous zone to the point above the ribbon where the luminous intensity starts to decrease is the apparent flame diameter (frame 30, fig. 2), an average over a number of points on each frame and over a number of frames. The numbers are at best relative on a rather indefinite scale because of constant exposure times and differences in energy-release rates producing some overexposure, and because of the difficulties of visually estimating intensities.

3277

EXPERIMENTAL RESULTS

Typical still photographs of burning magnesium ribbons are shown in figure 3. Figure 3(a) shows the ribbon twisted horizontally through the flame. Figure 3(b) is a medium exposure showing the ribbon less clearly than figure 3(a), but giving more emphasis to the flame structure. Figure 3(c) is a much heavier exposure; the igniter and the unburned ribbon are visible. Magnesium oxide smoke is seen streaming up from the fire, but the structural details of the flame are obliterated. The intense inner regions surrounding the ribbon in both figures 3(a) and (b) are surrounded by regions of somewhat lower luminosity which include, although only under the ribbon, a very thin region of high intensity. Figure 4 contains a schematic drawing indicating the various regions and shows microphotometer traces made across the paths indicated. The microphotometer traces indicate that, while the outer zone a is not an optical illusion, its intensity is not as high as that of the inner zone c.

The oxide ash left after a fire usually supported itself and spanned the gap. It maintained the general structure of the original ribbon, although it was fluffier for shorter burning times. For combustion in ordinary air, about 18 percent of the original magnesium remained in the ash as the oxide. The ash from the igniter thread also tended to preserve the structure of the original metal.

The experimental burning times are presented in figure 5. The time decreases with increasing oxygen concentration for all three diluents. The decrease is somewhat less for the nitrogen-inerted case than for the argon case, and is appreciably less for helium than for either argon or nitrogen. An indication of the precision of the data is given by vertical lines indicating the spread of the two to four individual tests which are included in each average value plotted as a datum point.

The effect of moisture in the surrounding atmosphere on burning time is indicated in figure 6. Amounts of water vapor, up to saturation at room temperature, were added to the mixtures of 21.5 and 43.7 percent oxygen in argon. The burning time decreases with increasing amounts of water, although the decrease in burning time per unit of added moisture is greatest for small quantities of water vapor. The precision of the measurements for low-moisture contents is generally poorer than the precision indicated in figure 5 for equivalent burning times. As a result, the faired curves are somewhat less significant than might be hoped; the qualitative effects are clear.

3277

DISCUSSION

One of the objectives of this investigation was to learn whether a vapor-phase or a surface reaction controls the process under examination. The following evidence seems to indicate that a gaseous reaction occurs:

(1) Distinct zones are visible in the photographs, somewhat like those of liquid hydrocarbon diffusion flames. (The outer luminous zone a, fig. 4, has tentatively been attributed to the recalescence of magnesium oxide.)

(2) The light intensity, as indicated on the microphotometer traces, was greater above and below the ribbon than right on it (fig. 4).

(3) The ribbon did not seem actually to liquify, although it did soften and twist; it supported itself on medium spans (for example, across the approximately 2.3 cm between the igniter and the bracket), although it sagged on somewhat broader spans. The ash retained the general shape of the original ribbon. While these properties might in part belong to the oxide deposited on the surface rather than to the magnesium alone, the observations suggest that the temperature at the metal surface is in the range between the melting (923° K) and the boiling (1393° K) points of magnesium, well below observed flame temperatures ($>3000^{\circ}$ K).

(4) An appreciable loss of magnesium from the ribbon occurred during the burning process, the oxide ash showed no indication of fusion, and the ash was fluffier for shorter burning times (faster rates). These observations suggest the evaporation of magnesium at a temperature well below that of the melting point of the oxide ($>2500^{\circ}$ K).

(5) Photographs of igniter threads burning in oxygen without ribbons showed flames of the same general size and shape as did threads burning under similar conditions in chlorine. To produce flames in chlorine, heat had to be supplied continuously to the igniter and its thread; the magnesium apparently melted. This observation suggests a metal volatilization process for the chlorine flame, and, hence, from the similarities of the photographs for the two cases, a vapor-phase mechanism for the formation of the oxide.

In view of the evidence for the occurrence of a vapor-phase process in the burning of magnesium, an attempt was made to compute burning rates, and, hence, burning times, by a method that has proved highly successful for single liquid fuel droplets. The two-region "stagnant film" approach of Spalding and later of Graves was adopted (ref. 19 and 21). Preliminary calculations (neglecting dissociation) suggested excessive temperatures ($T \cong 5 \times 10^4$ °K multiplied by the mole fraction of oxygen); however, experimental measurements suggested a flame temperature of about 3100° K (refs. 15 and 16), approximately the boiling point of magnesium oxide. Since the oxide is believed to dissociate almost completely upon vaporization (ref. 24), dissociation could not be treated by the technique of reference 21. Rather it was decided to abandon the concept of an infinitesimally thin flame front and to consider a finite reaction zone of high-temperature diffusion. The model is shown in cross section in figure 7. It consists of three concentric cylindrical zones, with boundaries designated A, B, B', and C. The metal is vaporized from the ribbon surface A at about the boiling point of magnesium. Then three zones AB, BB', and B'C are established:

3277

(1) A zone AB of radially increasing temperature; the metal vapor is heated and heat is conducted to the metal surface to vaporize more metal.

(2) A zone BB', a constant temperature reaction zone at the boiling point of magnesium oxide. Interdiffusion of the oxygen and magnesium occurs. The result is a chemical equilibrium between condensed oxide, magnesium vapor, and oxygen all at the boiling point of the magnesium oxide in a stagnant film of inert gas.

(3) A zone B'C of radially decreasing temperature, consisting of a stagnant film of inert gas with oxygen diffusing inward and being heated and with condensed oxide moving out and being cooled. [In the treatment of the spherical case, a steady-state solution is obtained as the radius of the C boundary approaches infinity; however, for the treatment of the cylindrical or flat-plate cases, a finite boundary condition is required.]

The general approach and the significant assumptions involved in the calculation will be indicated here. The symbols used and the details of the calculation are presented in appendixes A and B, respectively.

The physical assumptions are:

(1) The metal ribbon can be adequately treated with cylindrical geometry; end effects are neglected.

(2) The temperature does not exceed 3200° K; this follows from the assumption of complete dissociation of magnesium oxide upon vaporization.

(3) The regions of highest luminosity correspond to the reaction zone; specifically, the apparent flame diameter has been taken as the B' boundary. Some indication of the effect of assuming other boundary conditions will be given.

(4) The effects of free convection are neglected in setting up fuel-flow, oxygen-diffusion, and heat-transfer equations for the steady-state process.

3277

(5) The required thermal conductivities and diffusion coefficients may be calculated, as no experimental data exist for the high-temperature values required. The thermal conductivity of the gases in the AB zone is taken as that of magnesium vapor (Mg) and in the B'C zone as that of the appropriate inert gas. Diffusion in the BB' and B'C zones is considered as the diffusion of oxygen into a stagnant film of the appropriate inert gas.

(6) In the B'C zone, as in reference 25, the film thicknesses for heat and mass transfer are assumed to be equal.

(7) The pressure throughout the system is at 1 atmosphere.

The calculation of burning time is carried out by computing the burning rate in terms of fuel consumed in moles per second; this calculation requires simultaneous solution of a number of differential equations for fuel-flow rate, oxygen diffusion, and heat transfer. These are organized zone by zone and integrated using the boundary conditions presented in the following table:

Boundary	Radius, cm	Temperature, °K	Partial pressure of oxygen, atm
A	r_A(metal surface)	1393 (b.p. Mg)	
B	r_B(eliminated)	3200 (approx. b.p. MgO)	$p_B = 0$
B'	$r_{B'}$(luminous surface)	3200 (approx. b.p. MgO)	$p_{B'}$(calc.)
C	r_C(not used)	300 (ambient)	p_C(ambient)

The following equations, derived in appendix B in order to calculate burning times, are indicated here in the integrated forms finally employed in computation.

AB Zone. - The heat-transfer equation for the metal vapor zone AB is

$$\frac{W_f}{2\pi l} \ln \frac{r_B}{r_A} = \underline{B} \tag{1}$$

where $\underline{B}$ is a definite integral over the temperature range and involves the thermal conductivity and thermodynamic properties of the metal vapor; in practice, a graphical integration is performed.

B'C Zone. - The heat-transfer equation for the B'C zone is

$$\frac{W_f}{2\pi l} \ln \frac{r_C}{r_{B'}} = \underline{C} \tag{2}$$

where $\underline{C}$ is a definite integral over the temperature range and involves the properties of oxygen, the combustion products, and the inert gas; again, a graphical integration.

Also in B'C zone the oxygen diffusion equation is

$$\frac{W_f}{2\pi l} \ln \frac{r_C}{r_{B'}} = \underline{F} \left[\ln (1 - p_{B'}) \right] \tag{3}$$

where $\underline{F}$, a function of $\ln (1 - p_{B'})$, is a definite integral of the diffusion equation over the range of the partial pressure of oxygen.

When W_f is eliminated from equations (2) and (3), $\ln (1 - p_{B'})$ may be determined for each condition of inert and ambient oxygen concentration.

BB' Zone. - The oxygen diffusion equation in the BB' zone is

$$\frac{W_f}{2\pi l} \ln \frac{r_{B'}}{r_B} = \underline{B}' \left[\ln (1 - p_{B'}) \right] \tag{4}$$

where $\underline{B}'$ is a definite integral of the diffusion equation over the range of partial pressure of oxygen. When values of $\ln (1 - p_{B'})$ obtained by combining equations (2) and (3) are used, $\underline{B}'$ may be evaluated in equation (4).

From equations (1), (2), and (4), a series of expressions as derived in equation (B12), (appendix B), may be obtained, including

3277 2-CO

$$\frac{W_f}{2\pi l} = \frac{\underline{B} + \underline{B}'}{\ln \frac{r_{B'}}{r_A}} = \frac{\underline{B} + \underline{B}' + \underline{C}}{\ln \frac{r_C}{r_A}} = \frac{m}{M2\pi l t} \tag{5}$$

Then

$$t = 4.85 \times 10^{-5} \frac{\ln \frac{r_{B'}}{r_A}}{\underline{B} + \underline{B}'} \tag{6}$$

3277

or any of a number of similar expressions. The mass per unit length of the magnesium ribbon is 0.0074 gram per centimeter and the molecular weight of magnesium is 24.3. The definite integrals over temperature in the AB and the B'C zones, $\underline{B}$ and $\underline{C}$, respectively, are relatively small as compared with the definite integral over partial pressure of oxygen $\underline{B}'$ in the BB' zone for oxygen concentrations above 40 to 50 percent. Since $\underline{B}$, $\underline{B}'$, and $\underline{C}$ can be evaluated by equations (B5), (B7), and (B11) of appendix B (values are given in fig. 8), the burning time will be determined by the values assigned to the radii of the boundaries of the zones. The radius r_A is associated with the ribbon; in particular, the radius of a cylinder of equal surface area (0.1025 cm) has been adopted; an alternative is the use of the radius of equivalent cross section (0.0386 cm), and the difference in the result is an increase in computed burning time t by a factor of about 2. The radius $r_{B'}$ has been taken as one-half the apparent flame diameter; the data are shown in figure 9. Values have been taken as independent of oxygen concentration; in any case, the error of such an assumption will be insignificant on an absolute basis and of second-order effect on a relative basis. Moreover, it should be noted that while free convection has been neglected in the mathematical derivation, the position of this experimental boundary may be strongly affected by convection.

Figure 10 shows the effects on the computed burning time and zonal structure of the assumption that r_C, rather than $r_{B'}$, is properly represented by a constant diameter. Again, the effect in t on an absolute basis is small especially for oxygen concentrations above 40 to 50 percent; relative values of t are decreased to some extent in the lower ranges of oxygen concentration.

Although both experimental and computed burning times are averages, the averages are not taken in precisely the same way. There is reason to believe that the burning rate which is equivalent to the fuel flow W_f may be a function of r, and indeed equation (5) shows that it will be, unless the ratios of the diameters of the cylindrical zones remain constant. However, in the experiment a ribbon was used, and therefore

an assumption of constant surface area and, hence, constant effective r_A is plausible. In the calculation, the implicit assumption is that the cylinder is ignited over its entire length instantaneously and burns uniformly. In the experiment, the burning time includes time for the flame to spread along the ribbon and takes little account of the fact that some portions are completely burned out in less than the burning time; a rough estimate is that these effects increase the observed times by a factor of about 2 which may also have a second-order dependence on oxygen concentration.

3277
CO-2 back

The experimental 100-percent-oxygen value may better be considered as an upper limit than as a true value because of the large calculated effects of traces of inert gas and/or the possibility that heat-transfer processes take control for very short times. The behavior of the computed curve for very high oxygen concentrations is shown by the dashed portion between 90 and 100 percent in figure 11(a).

Figures 11(a), (b), and (c) show the results of carrying out the calculation outlined previously for each of the inert gases, argon, nitrogen, and helium, respectively. Each figure gives the appropriate experimental curve from figure 5, the calculated curve as obtained incorporating the assumptions and boundary conditions specified, and a normalized computed curve for comparison purposes. Normalization involved the multiplication of the computed curve by the ratio, (experimental value, 50 percent O_2)/(computed value, 50 percent O_2). The values of the ratio used are 2.13 for argon, 2.04 for nitrogen, and 2.72 for helium; the constant for the helium case depends significantly upon the oxygen concentration selected for the normalization procedure. As presented, no physical significance is attached to the ratio; however, factors of the magnitude involved could be obtained by decreasing r_A, by decreasing the high-temperature diffusion coefficient $D_{BB'}$, or by considering the spreading time of the flame.

The correct prediction of the effect of oxygen concentration is the matter of major significance here; that is, the prediction of correct relative rates. In addition, calculation of the proper order of magnitude for the actual time is gratifying; although the absolute agreement within a factor of 2.5 for argon and nitrogen must be deemed fortuitous.

The argon curves (fig. 11(a)) show the best fit between experiment and calculation, followed quite closely by the nitrogen case (fig. 11(b)). The somewhat less satisfactory agreement for nitrogen is most readily attributed to the fact that nitrogen is not truly inert in this process; magnesium nitride is known to form, and traces of ammonia were present after runs. Nitrogen acting as reactant would tend to reduce burning time at low oxygen concentrations as is observed. However, the close

agreement between the nitrogen and argon experimental curves shows that here those effects have been eliminated which in high-temperature slow-oxidation experiments cause magnesium to oxidize more rapidly in air than in pure oxygen (ref. 18). No significant difference was obtained in the calculated curves for nitrogen and argon. Although the nitrogen curve is very slightly disposed in the direction indicated by the experiments, the differences are small compared with the assumptions involved, particularly in the calculation of the high-temperature diffusion coefficients.

3277

The helium curve (fig. 11(c)) shows considerable departure from experiment at low oxygen concentrations (these mixtures are also of relatively low density compared with the others considered). A considerable part of this departure is no doubt due to the difficulties of computing thermal conductivities and diffusion constants for mixtures of constituents varying widely in molecular weight. Efforts to account for concentration effects on the properties involved are of doubtful validity and, in any case, show little improvement in the final results.

The calculations with the inert gases do predict that helium should show shorter burning times than argon and nitrogen and this prediction is in agreement with the experiments. In comparison, the effect of inert gases in reducing the burning velocities of homogeneous hydrocarbon flames appears as $N_2 > A > He$ (ref. 23); from this investigation, if there is an analogy between burning velocity and the reciprocal of the burning time, $N_2 \cong A \geqslant He$. However, here it is known that nitrogen is not completely inert and would tend to produce a shift in the direction observed; from $N_2 > A$ for the hydrocarbon case to $N_2 \cong A$ for the magnesium case. Furthermore in the homogeneous case, flame temperatures are not equal as has been assumed herein.

The effect of water is less satisfactorily explained in terms of the thermal and diffusional model presented. It would appear more probable that moisture affects the chemical or diffusion processes at either B or B' or at both boundaries than that it changes the gross properties within an entire zone. Water vapor produces an increase in the oxidation rate in these experiments as it did in the high-temperature slow-oxidation-rate studies on magnesium (ref. 18).

Nevertheless, in spite of certain anomalies between the experimental data and the computed burning times, the general agreement strongly supports the basic assumption of a vapor-phase reaction.

SUMMARY OF RESULTS

Magnesium ribbons were burned in mixtures of oxygen, 17 to 100 percent by volume, with argon, nitrogen, helium, and argon - water vapor.

Experimental burning times were determined, and some details of the physical mechanism of the combustion process have been investigated. The following results were obtained:

1. The burning time decreased sharply with increasing oxygen concentration.

2. The burning time in argon-oxygen mixtures decreased in the presence of moisture, with traces of water vapor showing the greatest effect.

3. A vapor-phase mechanism for the combustion of magnesium ribbons was very strongly indicated.

4. Stagnant-film concepts involving a reaction zone of finite thickness permitted the calculation of relative burning time in terms of the properties of the oxidizing atmosphere.

Lewis Flight Propulsion Laboratory
National Advisory Committee for Aeronautics
Cleveland, Ohio, September 27, 1954

3277

APPENDIX A

SYMBOLS

The following symbols are used in this report:

A, B, B', C	boundaries of zones, fig. 7
AB, BB', B'C	zones between appropriate boundaries
$\underline{B}$	definite integral over temperature in AB zone, eq. (B5), moles/(cm)(sec)
$\underline{B}'$	definite integral over partial pressure of oxygen in BB' zone, eq. (B11), moles/(cm)(sec)
$\underline{C}$	definite integral over temperature in B'C zone, eq. (B7), moles/(cm)(sec)
D	diffusion coefficient of oxygen, sq cm/sec
$\underline{F}$	definite integral over partial pressure of oxygen in B'C zone, eq. (B10), moles/(cm)(sec)
G_f	fuel flow per unit area, moles/(sq cm)(sec)
H	heat required for process per mole of fuel, cal
h_f, h_p, h_{O_2}	enthalpy of fuel, product, oxygen at T, cal/mole
$h_{f,A}$	enthalpy of fuel at $T_A = 1393^\circ$ K, cal/mole
$h_{p,C}$, $h_{O_2,C}$	enthalpy of product, oxygen at $T_C = 300^\circ$ K, cal/mole
k	thermal conductivity, cal/(sq cm)(sec)($^\circ$C/cm)
L	heat of vaporization of fuel at $T_C = 1393^\circ$ K, cal/mole
l	length of cylinder, cm
M	molecular weight of magnesium, 24.3 g/mole
m	mass of magnesium ribbon, g
n	number of moles per mole of fuel; stoichiometric relation
P	total pressure, atm

3277

p	partial pressure of oxygen, atm
Q	heat of combustion of fuel at $T_C = 300^\circ$ K, cal/mole
R	universal gas constant, 82.05 (cu cm)(atm)/($^\circ$C)(mole)
r	radius, cm
T	absolute temperature, $^\circ$K
t	computed burning time, sec
W_f	fuel flow, moles/sec
W_{O_2}	oxygen flow, moles/sec

APPENDIX B

PREDICTION OF BURNING TIMES FOR MAGNESIUM RIBBONS

The stagnant-film approach of Spalding (ref. 19) and Graves (ref. 21) is modified to include a finite reaction zone of high-temperature diffusion in place of an infinitesimally thin flame front. Three symmetrical, concentric zones surround a metal cylinder (fig. 7), the result of the assumption of no convection. The metal is assumed to reach the boiling point during ignition. The temperature of the reaction zone is assumed not to exceed 3200° K, approximately the boiling point of magnesium oxide; this assumption is based on the fact that magnesium oxide is believed to dissociate upon vaporization (ref. 24), and means essentially that the heat of reaction at the boiling point is equal to the negative of the heat of vaporization. The concentration of oxygen is assumed to be zero at the inner boundary of the reaction zone. The diffusion of magnesium vapor is not considered explicitly; it is assumed that the diffusion of oxygen is into a stagnant film of gas having the properties of the appropriate inert gas with a total pressure of 1 atmosphere throughout the system.

The burning time is calculated in terms of the fuel flow (burning rate) W_f; the differential equations are set up zone by zone and integrated using the boundary conditions indicated in the text. The thermodynamic data used were as follows: heat of combustion and heat of vaporization of magnesium (ref. 26), enthalpy of oxygen (ref. 27), enthalpy of solid magnesium oxide from heat-capacity data (ref. 28), and enthalpy of magnesium vapor from a heat capacity of $\frac{5}{2}R$. Diffusion constants were calculated by the methods of Hirschfelder, Curtiss, and Bird (ref. 29) and are presented in the following table:

Inert gas	$D_{BB'}$(3200° K), sq cm/sec	$D_{B'C}$(300° K), sq cm/sec	$\frac{k_{B'C}T}{D_{B'C}}$ (300° K), cal/cu cm
Argon	10.5	0.196	6.4×10^{-2}
Nitrogen	10.9	.207	6.8
Helium	38.2	.75	15.2

The thermal conductivities of the inert gases were also computed according to reference 29. For the thermal conductivity of magnesium vapor, values of the viscosity were obtained by the use of the Sutherland formula, with a Sutherland constant (2130) taken equal to 1.54 times the boiling point of magnesium and a diameter of 3.2×10^{-8} centimeters; thermal conductivities were obtained from viscosities by the Eucken relation (ref. 30). Figure 12 shows the values of the thermal conductivities employed.

3277

Consider the rates at which fuel and oxygen are consumed in the steady state by the reaction $Mg + \frac{1}{2} O_2 \rightarrow MgO$:

$$G_f = \frac{W_f}{2\pi r l} = \frac{-W_{O_2}}{2\pi r l n_{O_2}} \tag{B1}$$

The negative sign signifies that fuel and oxygen are transferred in opposite directions.

The equation for the diffusion of a single gas through a stagnant film (ref. 31)

$$\frac{W_{O_2}}{2\pi r l} = - \frac{DP}{RT} \frac{1}{(P - p)} \frac{dp}{dr} \tag{B2}$$

may be applied in the various zones as follows:

Zone AB:

$$\frac{dp}{dr} = 0 \text{ and } W_{O_2} = 0$$

Zone BB':

$D = D_{BB'}$, the diffusion constant for oxygen into the appropriate inert gas

Zone B'C:

$D = D_{B'C}$ the diffusion constant for oxygen into the appropriate inert gas

The heat-transfer equation

$$HW_f = - 2\pi r l k \frac{dT}{dr} \tag{B3}$$

where H is the heat requirement per mole of fuel, may be applied in various zones as follows:

Zone AB:

$H = L + h_f - h_{f,A}$

$k = k_{AB}$ the thermal conductivity of magnesium vapor, Mg

HW_f is negative since heat is conducted inwardly.

Zone BB':

dT/dr is zero since the zone is assumed to be at the boiling point of magnesium oxide; H is also equal to zero.

Zone B'C:

$$H = Q - n_p (h_p - h_{p,C}) + n_{O_2} (h_{O_2} - h_{O_2,C})$$

$k = k_{B'C}$ the thermal conductivity of the appropriate inert gas (A, N_2, He)

HW_f is positive since heat is conducted outwardly.

The details of the application of equations (B1), (B2), and (B3) are presented for each zone as follows:

AB Zone. - The heat-transfer equation in zone AB is

$$\left[L + h_f - h_{f,A}\right] W_f = k_{AB}\, 2\pi r l \frac{dT}{dr} \tag{B4}$$

The term in brackets is the heat which must be conducted per mole inward from the reaction zone to vaporize the metal and raise the metal vapor to the temperature T, assuming the metal reaches its boiling point during ignition. The area of the cylinder is $2\pi r l$. The heat effects involved in the passage of some magnesium oxide to the ribbon in the experiment have been neglected.

Equation (B4) upon rearranging, applying the boundary conditions at A and B, and integrating yields

$$\frac{W_f}{2\pi l} \ln \frac{r_B}{r_A} = \int_{r_A}^{r_B} \frac{W_f}{2\pi r l}\, dr = \int_{T_A = 1393}^{T_B = 3200} \frac{k_{AB}}{\left[L + h_f - h_{f,A}\right]}\, dT \equiv \underline{B} \tag{B5}$$

3277

The graphical integration used here to calculate $\underline{B}$ is independent of the properties of the surrounding atmosphere.

B'C Zone. - The heat-transfer equation in zone B'C is

$$\left[Q - n_p(h_p - h_{p,C}) + n_{O_2}(h_{O_2} - h_{O_2,C})\right] W_f = - k_{B'C}\, 2\pi r l \frac{dT}{dr} \qquad (B6)$$

The term in brackets is the heat which must be transferred outward from the reaction zone in the combustion of 1 mole of fuel. The dissociation of oxygen (about 10 percent at 3200° K) is neglected. All magnesium oxide is assumed to pass outward through B'C zone for this heat balance.

Equation (B6) upon rearranging, applying the boundary conditions at B' and C, and integrating gives

$$\frac{W_f}{2\pi l} \ln \frac{r_C}{r_{B'}} = \int_{T_C = 300}^{T_{B'} = 3200} \frac{k_{B'C}}{\left[Q - n_p(h_p - h_{p,C}) + n_{O_2}(h_{O_2} - h_{O_2,C})\right]} dT \equiv \underline{C} \qquad (B7)$$

The definite integral $\underline{C}$ may be obtained graphically but has not been used explicitly because of physical assumption (3) in the text which identifies the apparent flame diameter with the B' boundary.

The equation for the diffusion of oxygen through the stagnant film in the B'C zone is

$$\frac{W_f}{2\pi r l} = - \frac{W_{O_2}}{2\pi r l n_{O_2}} = \frac{D_{B'C} P}{n_{O_2} RT} \frac{1}{(P - p)} \frac{dp}{dr} \qquad (B8)$$

Elimination of W_f from equations (B6) and (B8), which implicitly assumes that the film thicknesses for heat and mass tranfer are equal, produces

$$\frac{-k_{B'C}\, n_{O_2} \frac{RT}{D_{B'C}}}{\left[Q - n_p(h_p - h_{p,C}) + n_{O_2}(h_{O_2} - h_{O_2,C})\right]} dT = \frac{P}{(P - p)} dp \qquad (B9)$$

Since k and D/T have approximately the same temperature dependence, kT/D may be considered a constant (table in this section). Equation (B9) upon integrating, applying the appropriate boundary conditions at B' and C, and imposing the condition that P = 1 atmosphere yields

3277
CO-3 back

$$\int_{T_C = 300}^{T_{B'} = 3200} \frac{dT}{\left[Q - n_p(h_p - h_{p,C}) + n_{O_2}(h_{O_2} - h_{O_2,C})\right]}$$

$$= \frac{D_{B'C}P}{k_{B'C}\, n_{O_2} RT} \ln \frac{1 - p_{B'}}{1 - p_C} \equiv \frac{\underline{F}}{k_{B'C}} \qquad \text{(B10)}$$

Evaluating the left side graphically gives values of $\ln (1 - p_{B'})$ in terms of the properties of the surrounding atmosphere.

BB' Zone. - The equation for oxygen diffusion in the BB' zone upon integration and application of the boundary conditions at B and B' (including $p_B = 0$) and the condition $P = 1$ yields

$$\frac{W_f}{2\pi l} \ln \frac{r_{B'}}{r_B} = \frac{-D_{BB'}P}{n_{O_2} RT} \ln (1 - p_{B'}) \equiv \underline{B}' \qquad \text{(B11)}$$

The definite integral $\underline{B}'$ may be evaluated directly with values of $\ln (1 - p_{B'})$ obtained from equation (B10). The temperature throughout the BB' zone is taken as 3200° K. Values for $D_{BB'}$ are taken as those for oxygen diffusing into the appropriate inert gas; the assumption is that the effects of magnesium vapor will be negligible or, at least, about the same in every case.

Then, from equations (B5), (B7), and (B11), a series of expressions for W_f may be obtained:

$$\frac{W_f}{2\pi l} = \frac{\underline{B}}{\ln \frac{r_B}{r_A}} = \frac{\underline{B}'}{\ln \frac{r_{B'}}{r_B}} = \frac{\underline{C}}{\ln \frac{r_C}{r_{B'}}} = \frac{\underline{B} + \underline{B}'}{\ln \frac{r_{B'}}{r_A}} = \frac{\underline{B} + \underline{B}' + \underline{C}}{\ln \frac{r_C}{r_A}} = \frac{\underline{B}' + \underline{C}}{\ln \frac{r_C}{r_B}} \qquad \text{(B12)}$$

In addition to the relatively simple treatment presented, the more complex equations (ref. 31) for the diffusion of two vapors (here magnesium and oxygen through the inert gas) through a stagnant film were tentatively considered for the reaction zone. In this procedure, a partial pressure for magnesium of 0.9 atmosphere at the B boundary was assumed; this implies a temperature at the metal surface slightly below the boiling point of magnesium. The results of preliminary calculations

3277

indicate decreased values for $\underline{B}'$, although the dependence of $\underline{B}'$ on oxygen concentration remains about the same. The over-all effect appears to be a somewhat decreased oxygen dependence in the regions of oxygen concentration below about 50 to 60 percent, a somewhat increased dependence upon oxygen concentration in the regions above about 80 percent, and a general increase in the calculated burning times. Such a solution still involves certain approximations and increases the complexity of the calculations appreciably without assurance of increased accuracy. A complete solution of the problem, including magnesium-vapor diffusion within the AB zone, is far more complex and is not warranted by the available data.

3277

REFERENCES

1. Langmuir, Irving: Chemical Reactions at Low Pressures. Jour. Am. Chem. Soc., vol. 37, no. 5, May 1915, pp. 1139-1167.

2. Gulbransen, Earl A., and Andrew, Kenneth F.: Reactions of Artificial Graphite. Ind. and Eng. Chem., vol. 44, no. 5, May 1952, pp. 1034-1038; see also pp. 1039-1051.

3. Arthur, J. R., and Bangham, D. H.: The Mechanism of Energy Release in the Combustion of Solid Carbonaceous Fuels. Jour. chim. phys., T. 47, no. 5-6, May-June, 1950, pp. 559-562.

4. Davis, H., and Hottel, H. C.: Combustion Rate of Carbon. Ind. and Eng. Chem., vol. 26, no. 8, Aug. 1934, pp. 889-892.

5. Kuchta, J. M., Kant, A., and Damon, G. H.: Combustion of Carbon in High Temperature, High Velocity Air Streams. Ind. and Eng. Chem., vol. 44, no. 7, July 1952, pp. 1559-1563.

6. Arthur, J. R., Bangham, D. H., and Bowring, J. R.: Kinetic Aspects of the Combustion of Solid Fuels. Third Symposium on Combustion and Flame and Explosion Phenomena, The Williams & Wilkins Co. (Baltimore), 1949, pp. 466-475.

7. Arthur, J. R., Bangham, D. H., and Crone, H. G.: Topochemistry of Fuel Beds. Ind. and Eng. Chem., vol. 43, no. 2, Feb. 1951, pp. 525-528.

8. Foster, John F.: Production of Water Gas from Pulverized Coal. Ind. and Eng. Chem., vol. 40, no. 4, Apr. 1948, pp. 586-592. (See also additional papers from Symposium on Production of Synthesis Gas, pp. 558-641.)

9. Hazard, H. R., and Buckley, F. D.: Experimental Combustion of Pulverized Coal at Atmospheric and Elevated Pressures. Trans. A.S.M.E., vol. 70, no. 6, Aug. 1948, pp. 729-737.

10. Muraour, H., et Aunis, G.: Sur la relation entre la température d'explosion d'une poudre et sa vitesse de combustion. Chimie et industrie, T. 67, no. 6, June 1952, pp. 920-926.

11. Grosse, Aristid V., and Conway, Joseph B.: The Combustion of Metals. First Tech. Rep., High Temperature Proj., Res. Inst. of Temple Univ., Oct. 15, 1951. (Contract N9-onr 87301, Office Naval Res.)

12. Hartmann, Irving: Recent Research on the Explosibility of Dust Dispersons. Ind. and Eng. Chem., vol. 40, no. 4, Apr. 1948, 752-758.

13. Cassel, H. M., Das Gupta, A. K., and Guruswamy, S.: Factors Affecting Flame Propagation Through Dust Clouds. Third Symposium on Combustion and Flame and Explosion Phenomena, The Williams & Wilkins Co. (Baltimore), 1949, pp. 185-190.

14. Wolfhard, H. G., and Parker, W. G.: Emissivity of Small Particles in Flames. Nature, vol. 162, no. 4111, Aug. 1948, p. 259.

15. Wolfhard, H. G., and Parker, W. G.: Temperature Measurements of Flames Containing Incandescent Particles. Proc. Phys. Soc. (London), sec. B, vol. 62, pt. 8, no. 356B, Aug. 1, 1949, pp. 523-529.

16. Scartazzini, Hubert: Combustion du magnésium en poudre dans l'oxygéne. Comptes Rendus, T. 230, Jan. 1950, pp. 97-98.

17. Gulbransen, Earl A.: Kinetic and Structural Factors Involved in Oxidation of Metals. Ind. and Eng. Chem. vol. 41, no. 7, July 1949, pp. 1385-1391.

18. Terem, Haldun N.: Sur la cinétique de l'oxydation du magnésium. Comptes Rendus, T. 226, Mar. 1948, pp. 905-906.

19. Spalding, D. B.: Combustion of Fuel Particles. Fuel, vol. XXX, no. 6, June 1951, pp. 121-130.

20. Godsave, G. A. E.: Studies of the Combustion of Drops in a Fuel Spray - The Burning of Single Drops of Fuel. Fourth Symposium (International) on Combustion, The Williams & Wilkins Co. (Baltimore), 1953, pp. 819-830.

21. Graves, Charles C.: Combustion of Single Isooctane Drops in Various Quiescent Oxygen-Nitrogen Atmospheres. Proc. Third Midwestern Conf. on Fluid Mech., Univ. Minnesota, 1953, pp. 759-778.

3277

22. Spalding, D. B.: Combustion of Liquid Fuel in a Gas Stream, Pt. II. Fuel, vol. XXIX, no. 2, 1950, pp. 25-32.

23. Mellish, C. E., and Linnett, J. W.: The Influence of Inert Gases on Some Flame Phenomena. Fourth Symposium (International) on Combustion, The Williams & Wilkins Co. (Baltimore), 1953, pp. 407-420.

24. Brewer, Leo: The Thermodynamic Properties of the Oxides and Their Vaporization Processes. Chem. Rev., vol. 52, no. 1, Feb. 1953, pp. 1-75.

25. Spalding, D. B.: Combustion of Liquid Fuel in a Gas Stream, Pt I. Fuel, vol. XXIX, no. 1, Jan. 1950, pp. 2-7.

26. Rossini, Frederick D., et al: Selected Values of Chemical Thermodynamic Properties. Circular No. 500, Dept. Commerce, Nat. Bur. Standards, Feb. 1952.

27. Huff, Vearl N., Gordon, Sanford, and Morrell, Virginia E.: General Method and Thermodynamic Tables for Computation of Equilibrium Composition and Temperature of Chemical Reactions. NACA Rep. 1037, 1951. (Supersedes NACA TN's 2113 and 2161.)

28. Perry, John H., ed.: Chemical Engineers' Handbook. Third ed., McGraw-Hill Book Co., Inc., 1950, p. 221.

29. Hirschfelder, Joseph O., Curtiss, Charles F., and Bird, R. Byron: Molecular Theory of Gases and Liquids. John Wiley & Sons, Inc., 1954, ch. 8.

30. Chapman, Sydney, and Cowling, T. G.: The Mathematical Theory of Non-Uniform Gases. Cambridge Univ. Press, 1939.

31. Sherwood, Thomas K.: Absorption and Extraction. McGraw-Hill Book Co., Inc., 1937.

3277

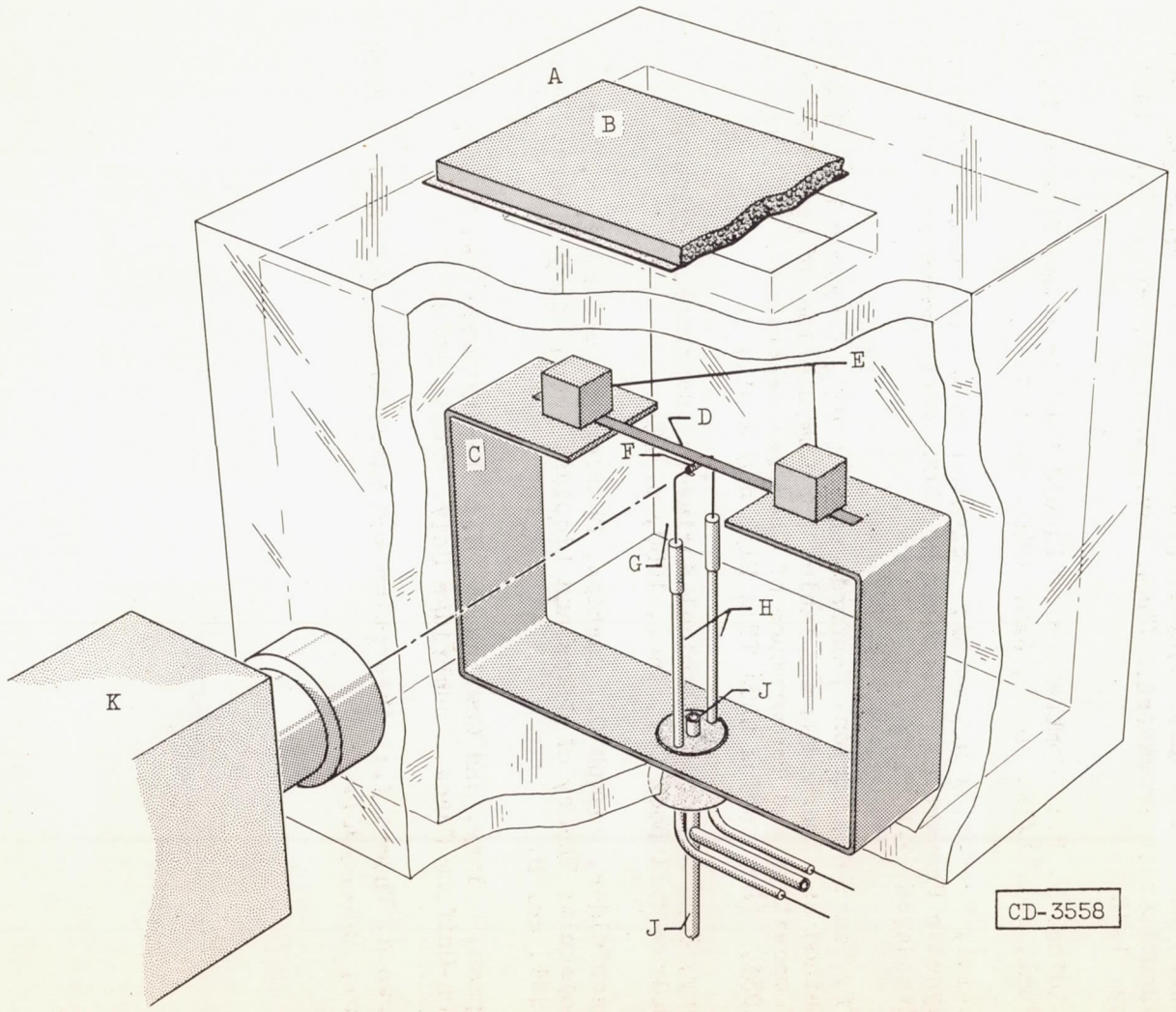

A Box
B Cover
C Bracket
D Ribbon
E Weights
F Thread
G Heater
H Electrodes
J Filling tube
K Camera

Figure 1. - Magnesium ribbon burning apparatus.

3277
CO-4

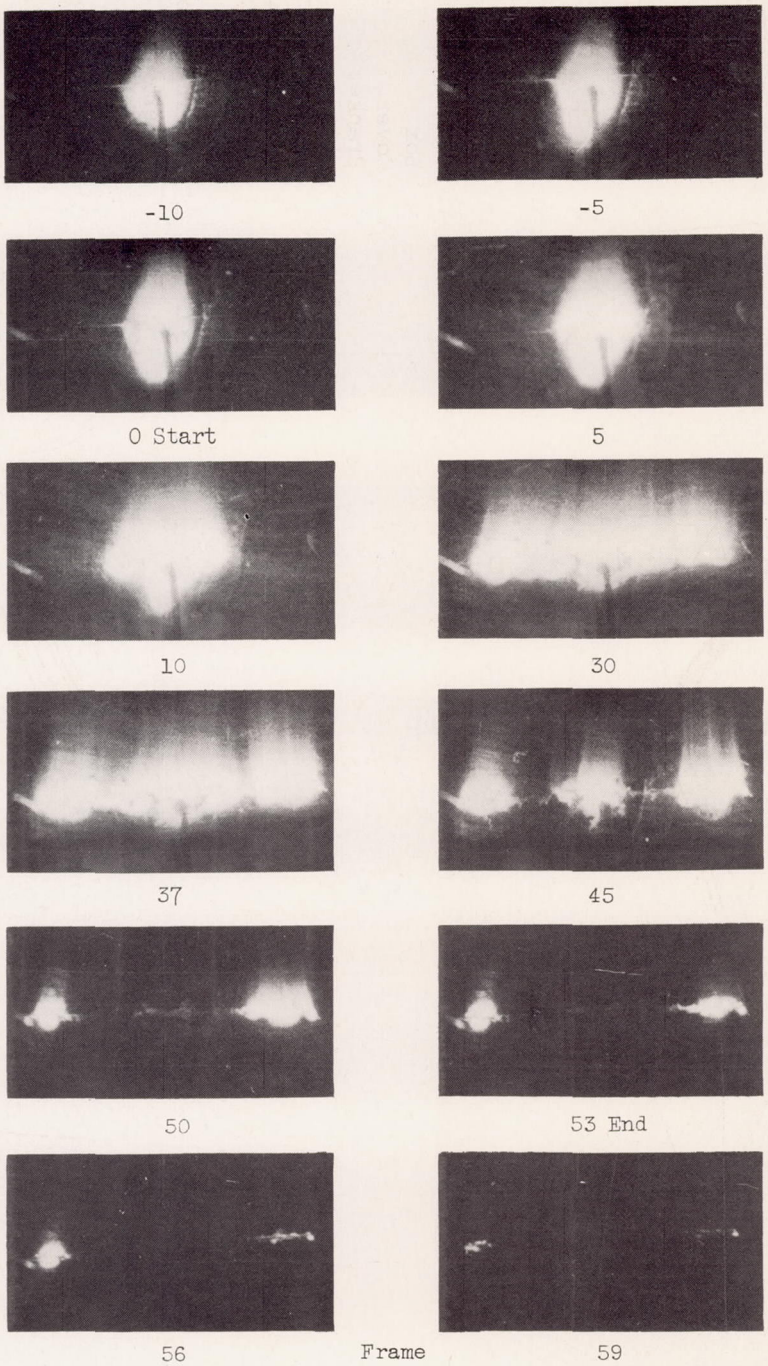

Figure 2. - Selected frames from motion pictures of burning magnesium ribbon.

3277

(a) Short.

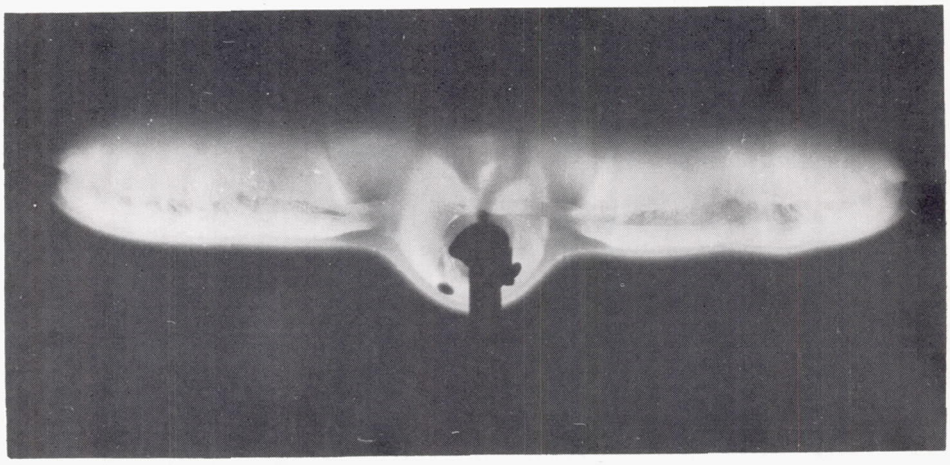

(b) Medium.

C-36771

(c) Long.

Figure 3. - Burning magnesium ribbon, increasing exposures top to bottom.

CO-4 back 3277

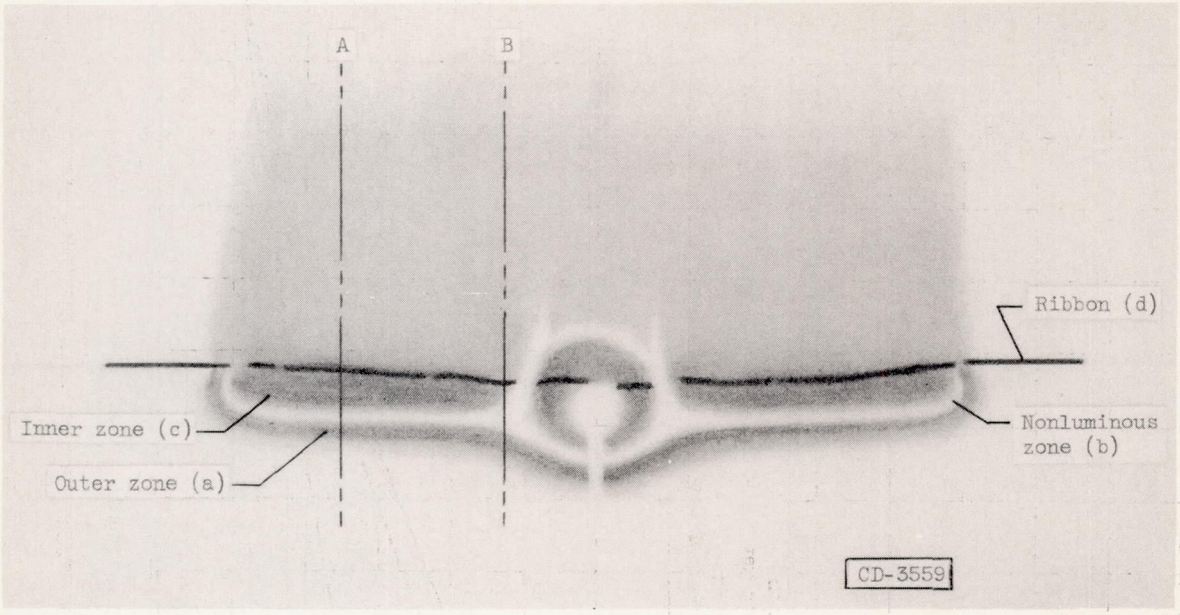

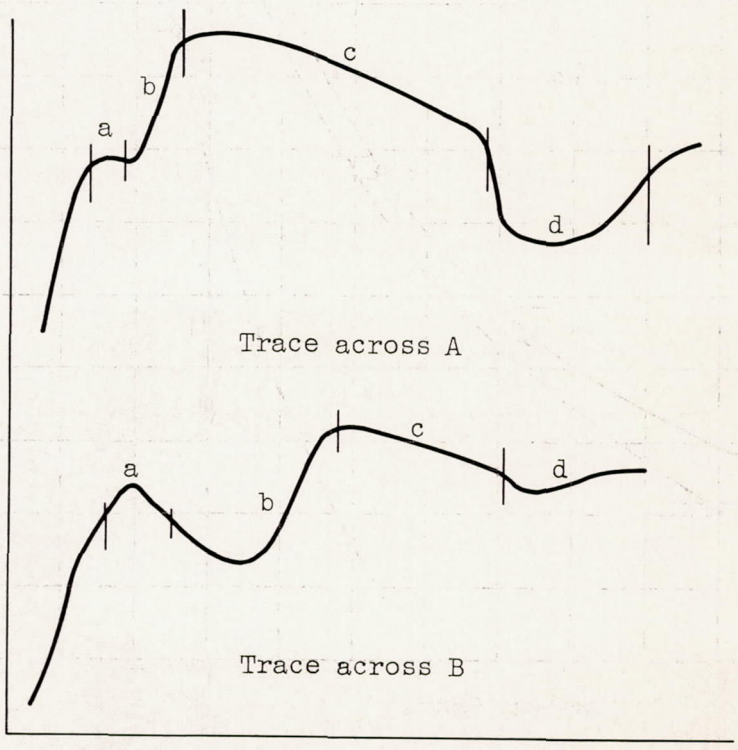

Figure 4. - Schematic drawing of flame; microphotometer traces.

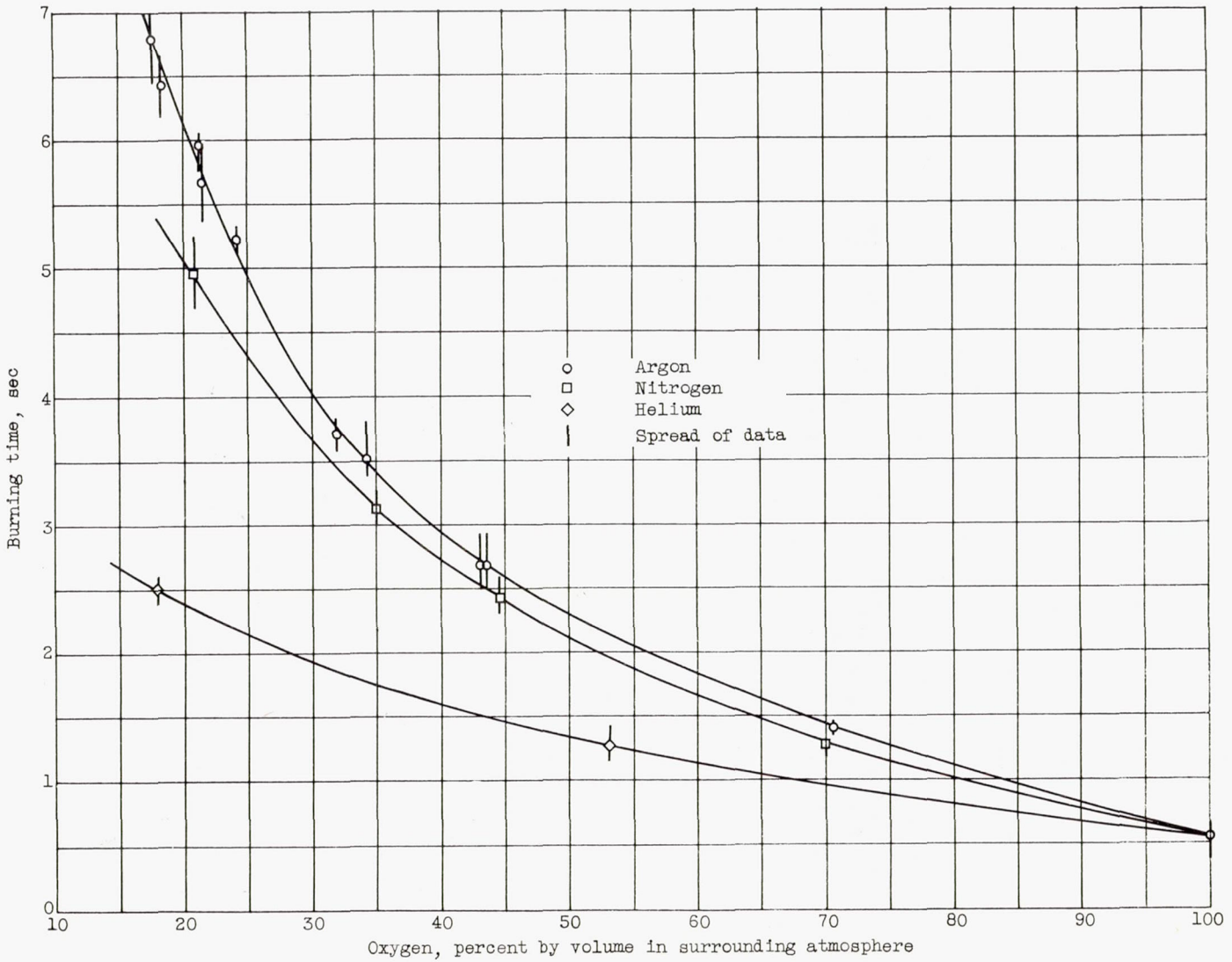

Figure 5. - Variation of burning time with oxygen concentration and inert gas.

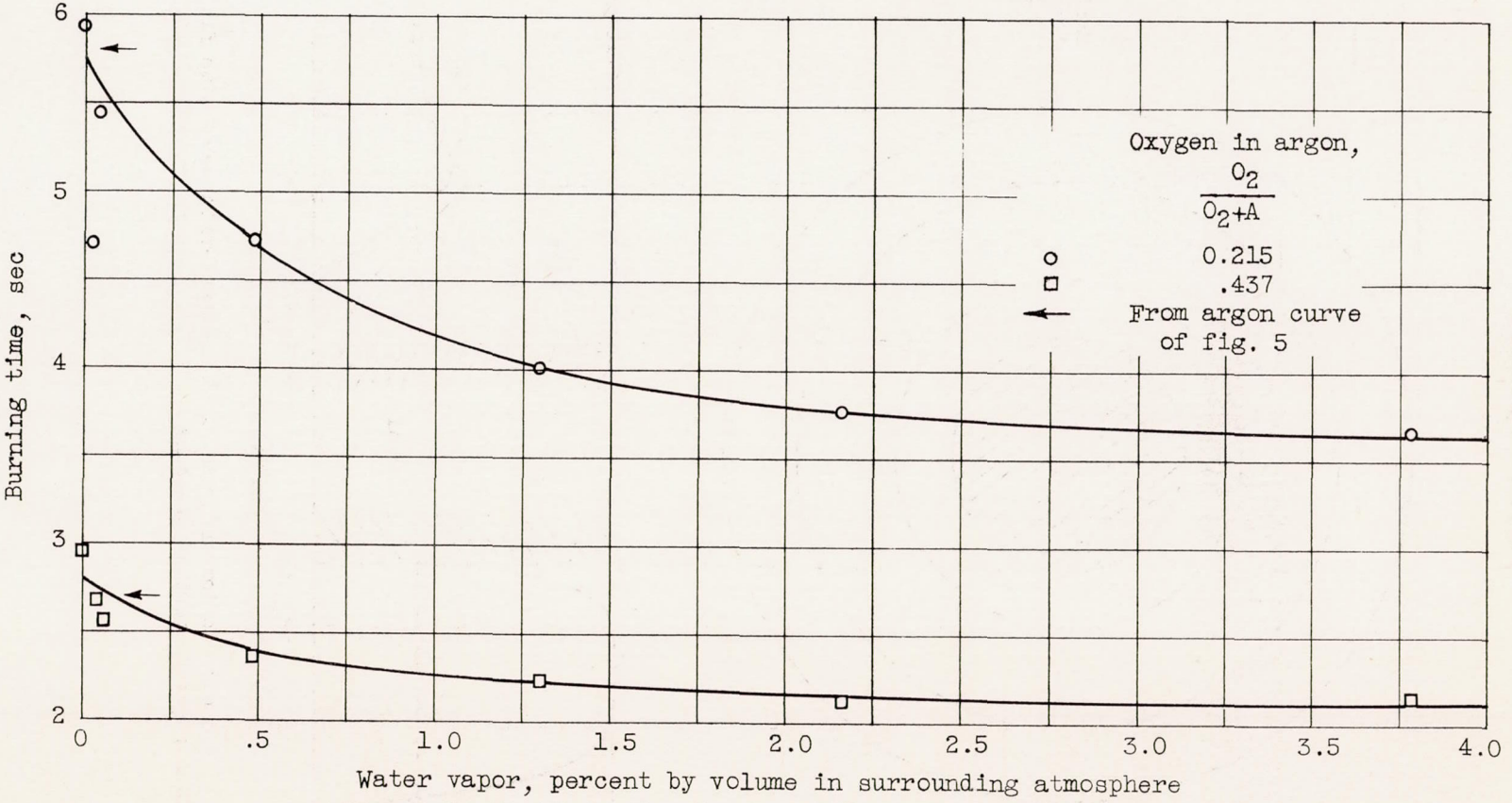

Figure 6. - Variation of burning time with water concentration.

3277

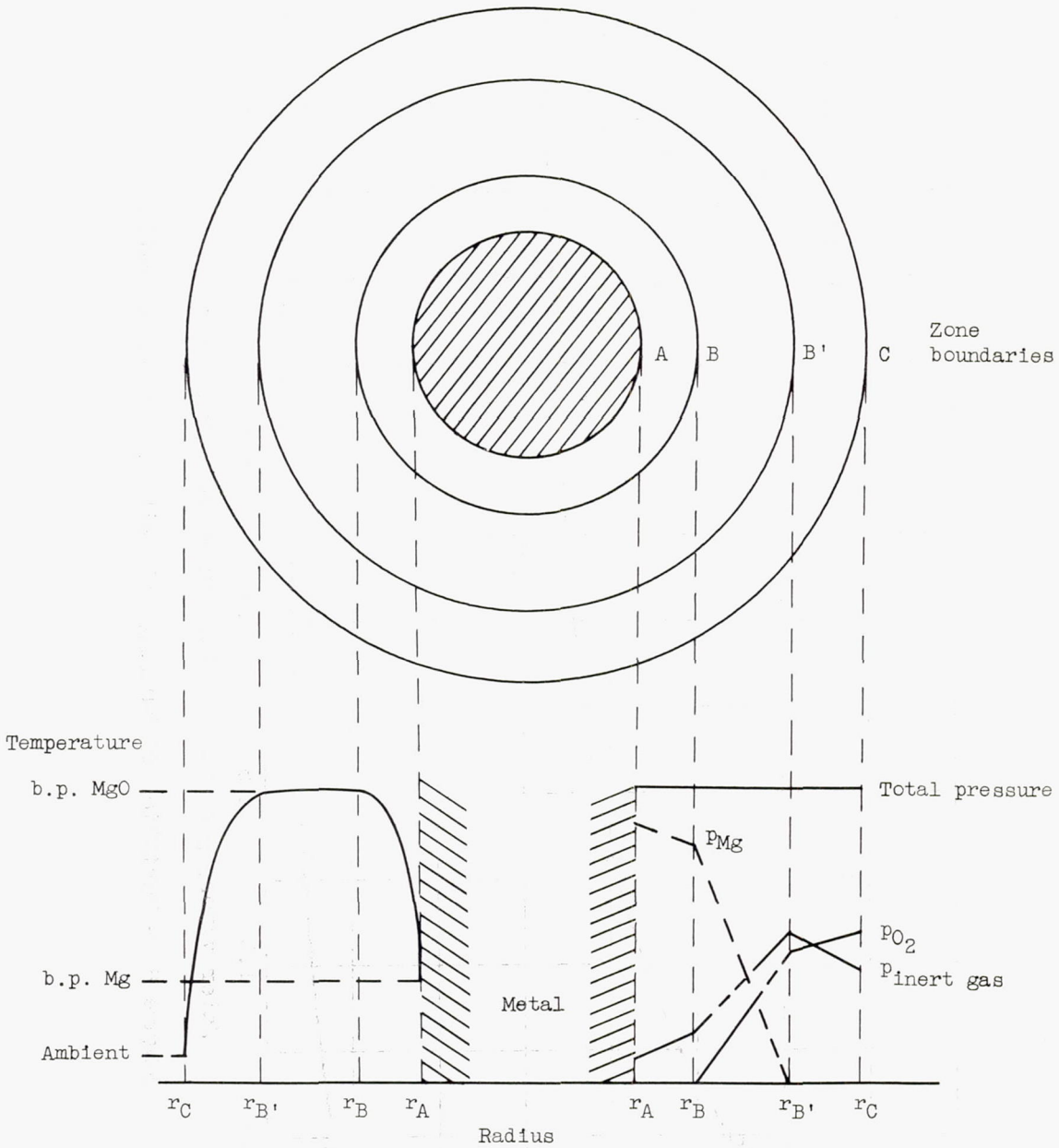

Figure 7. - Cross section of cylindrical stagnant-film model with finite reaction zone; p, partial pressure.

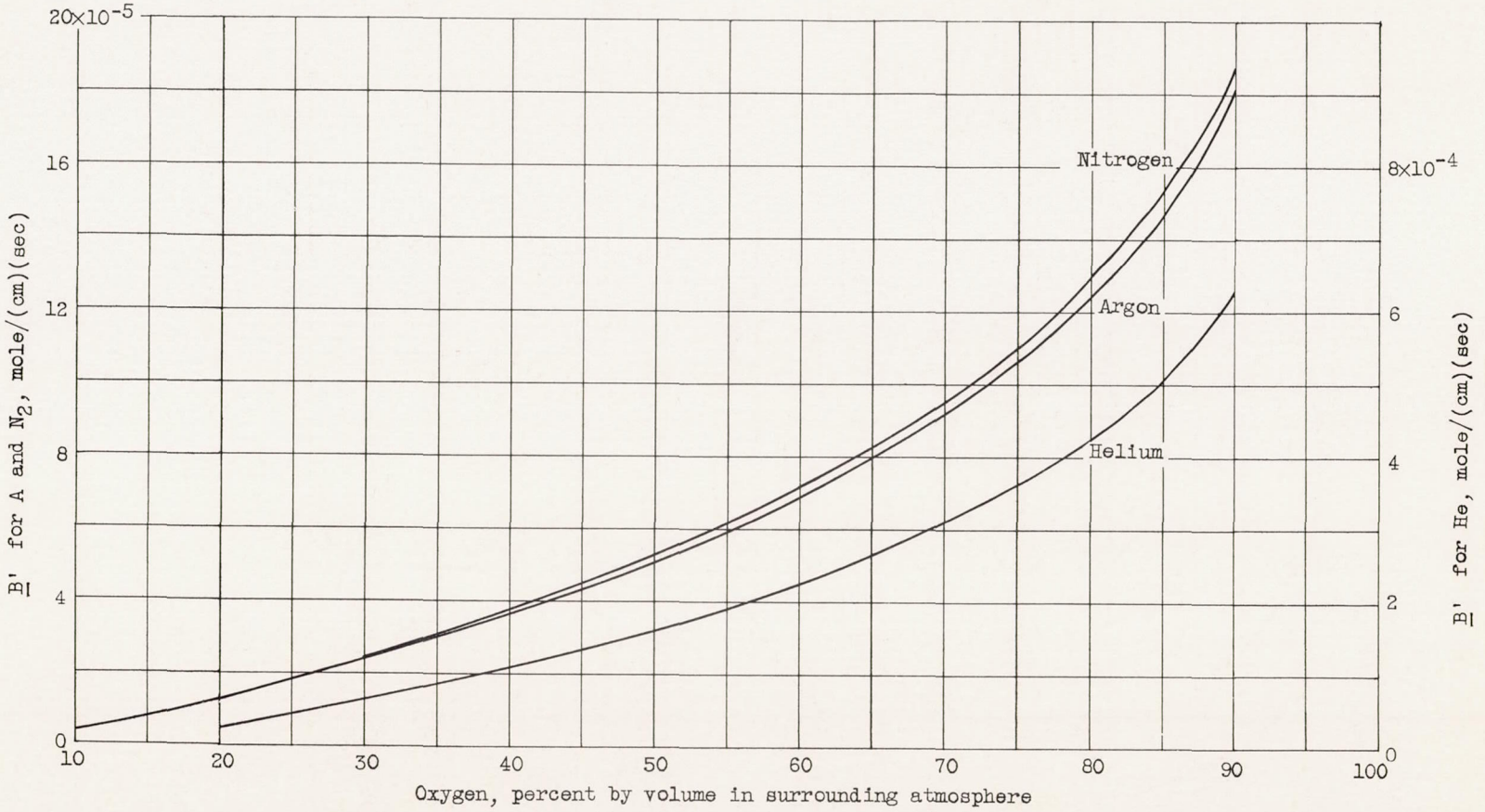

Figure 8. - Values of definite integrals defined in equations (B5), (B7), and (B11). $\underline{B}$, 0.48×10^{-5} mole per centimeter per second; $\underline{C}$ for argon, nitrogen, and helium: 0.30, 0.33, and 2.52×10^{-5} moles per centimeter per second, respectively.

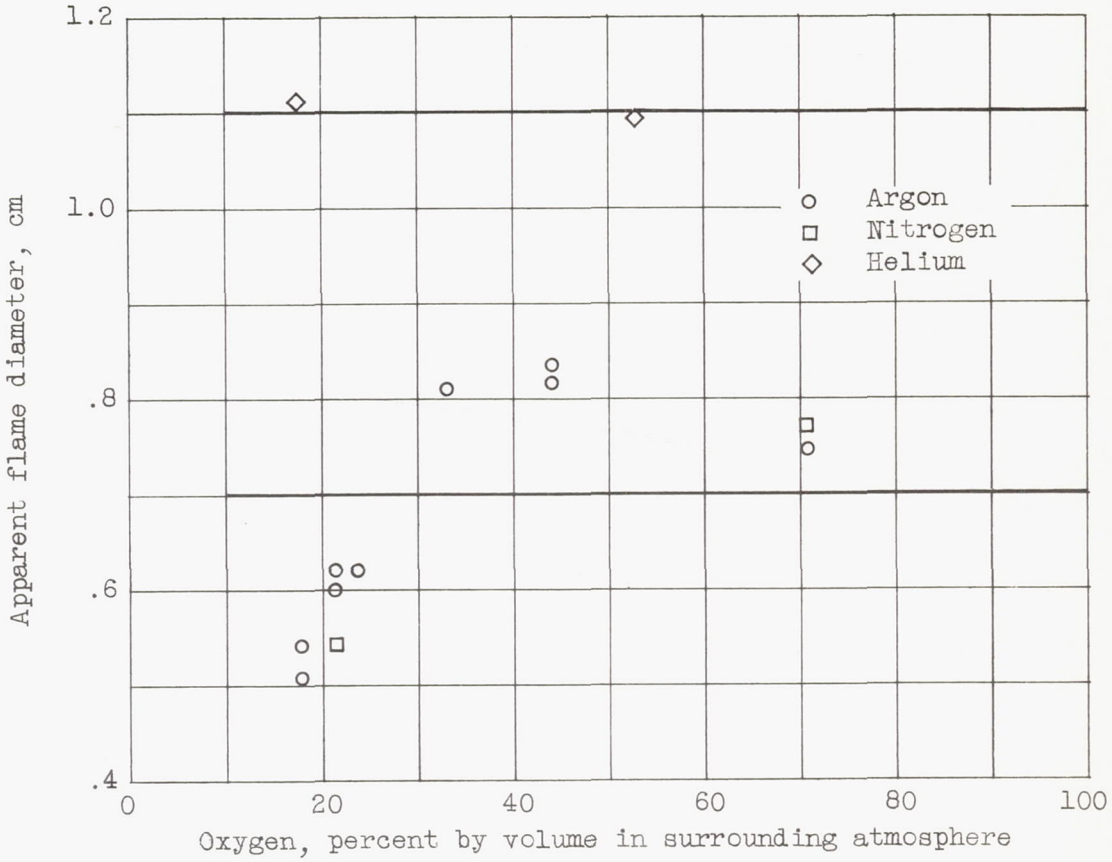

Figure 9. - Variation of apparent flame diameter with oxygen concentration and inert gas.

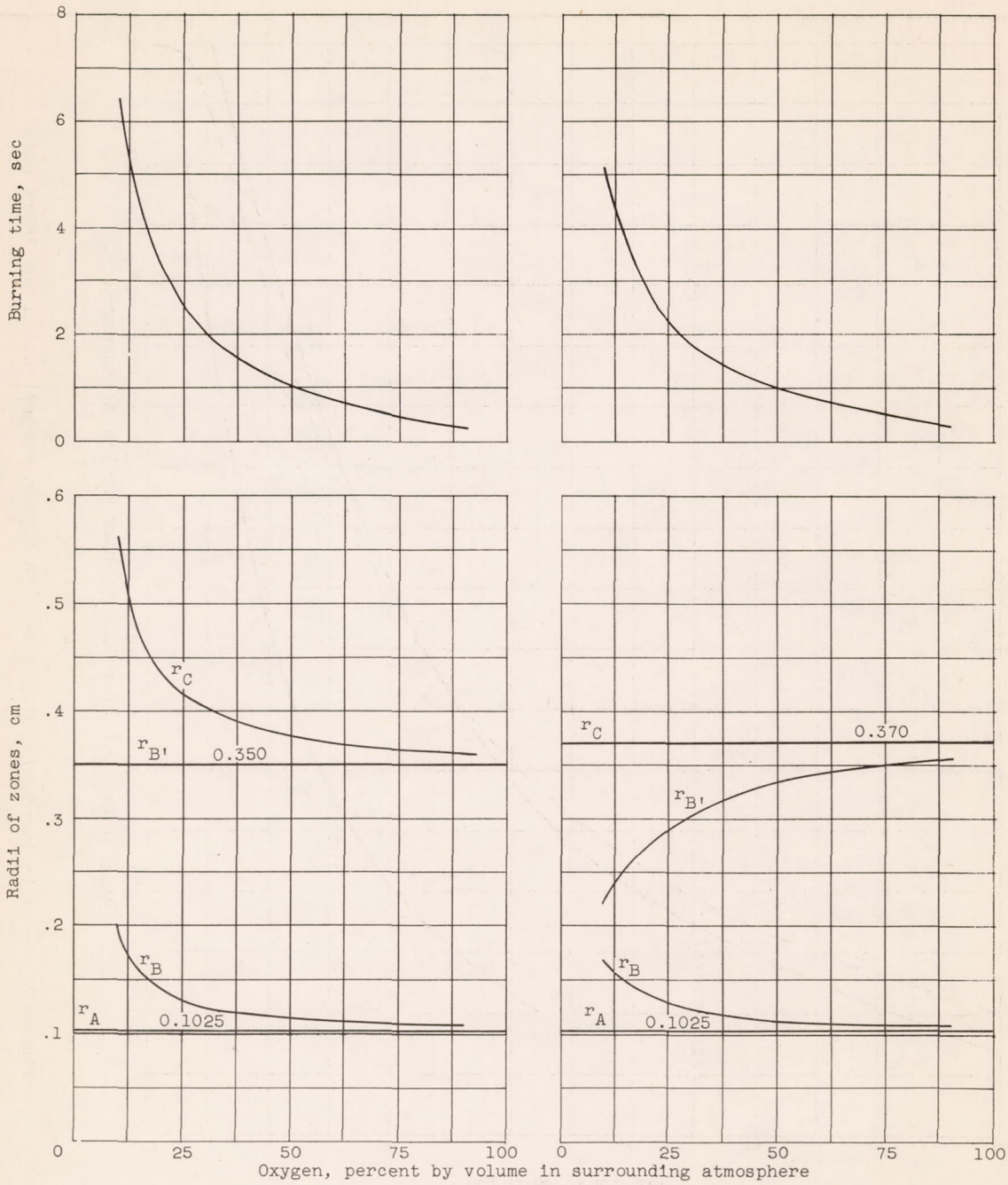

(a) $r_{B'}$ held constant. (b) r_C held constant.

Figure 10. - Effect of boundary conditions on zonal structure and burning time.

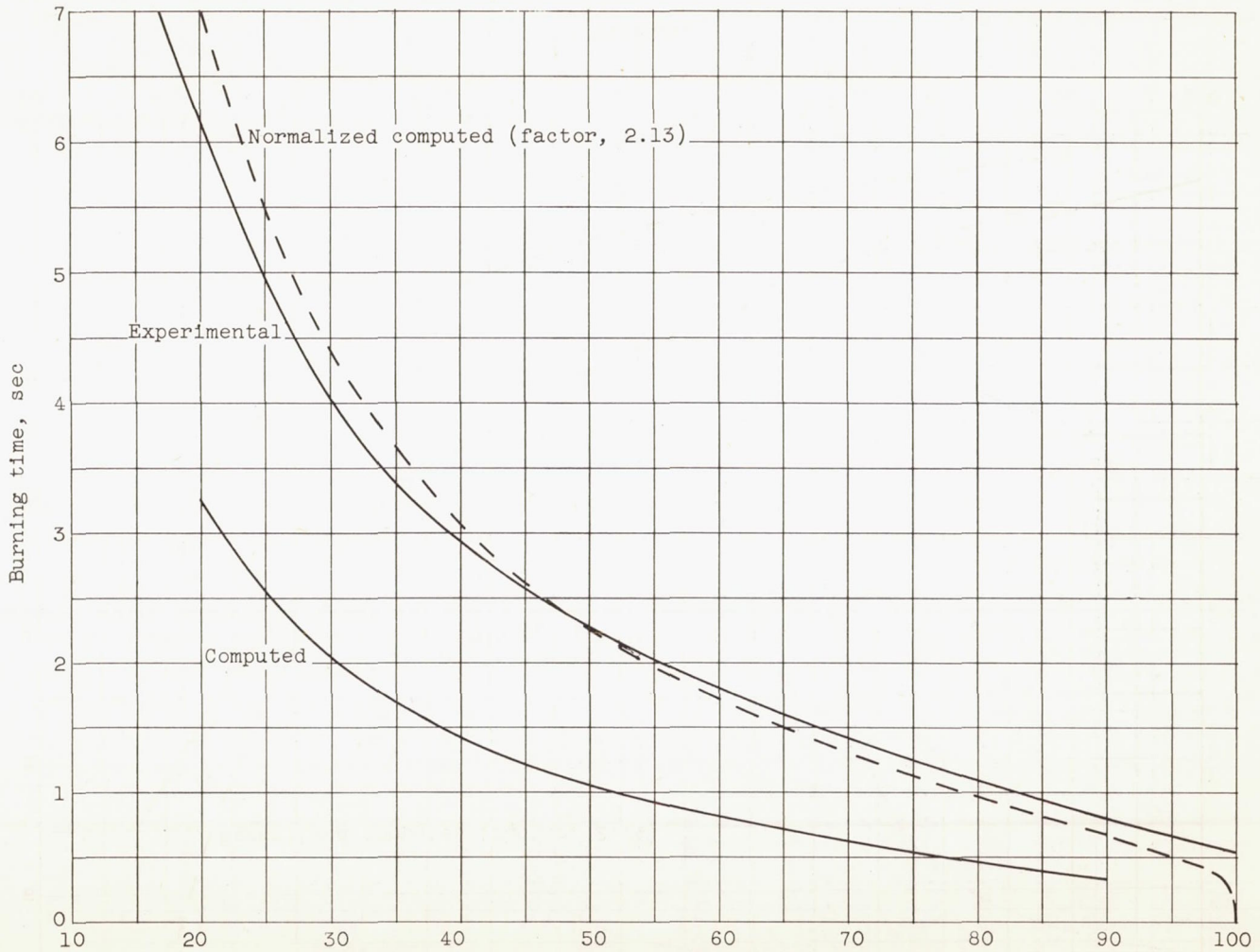

(a) Argon.

Figure 11. - Variation of burning time with oxygen concentration and inert gases.

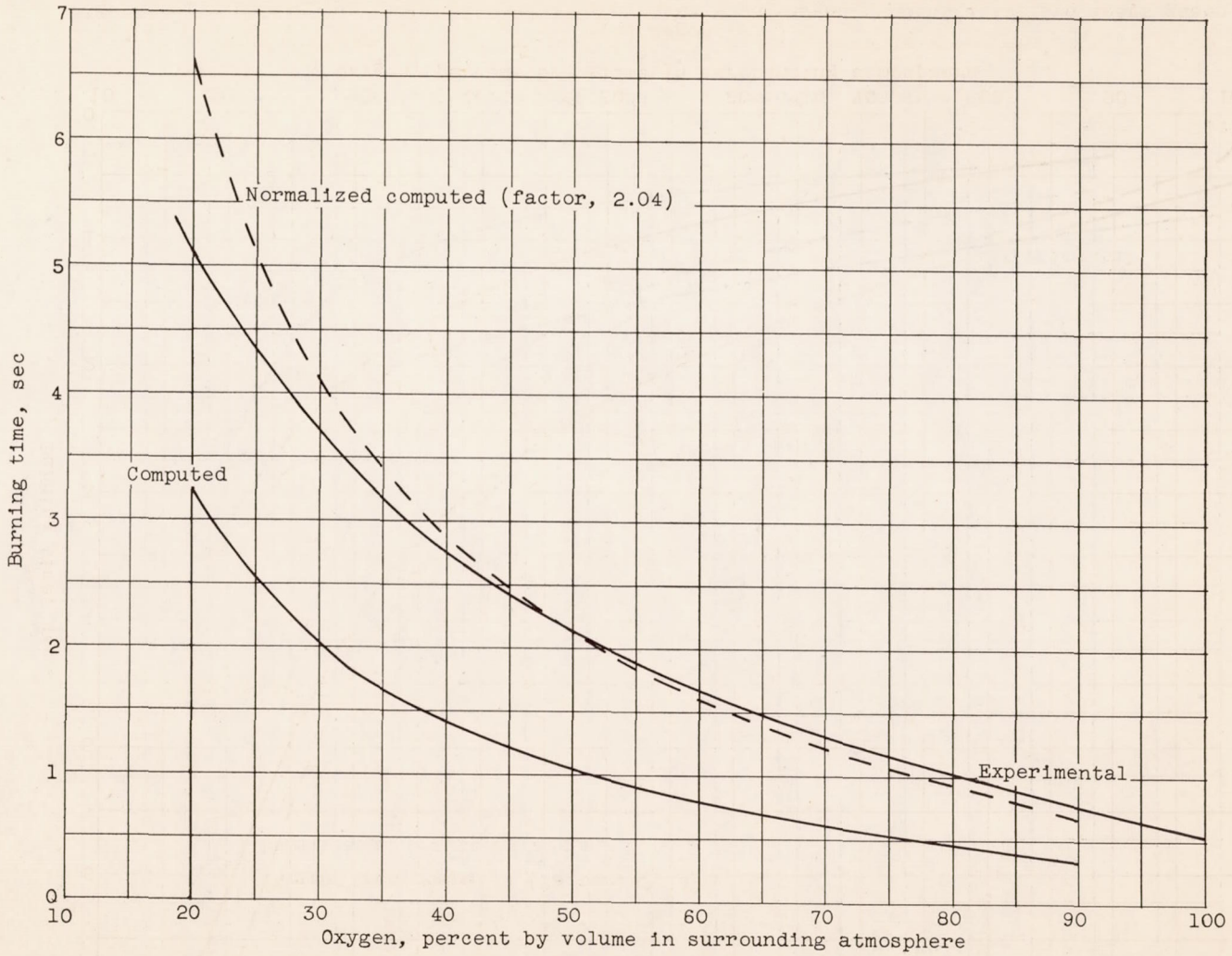

(b) Nitrogen.

Figure 11. - Continued. Variation of burning time with oxygen concentration and inert gases.

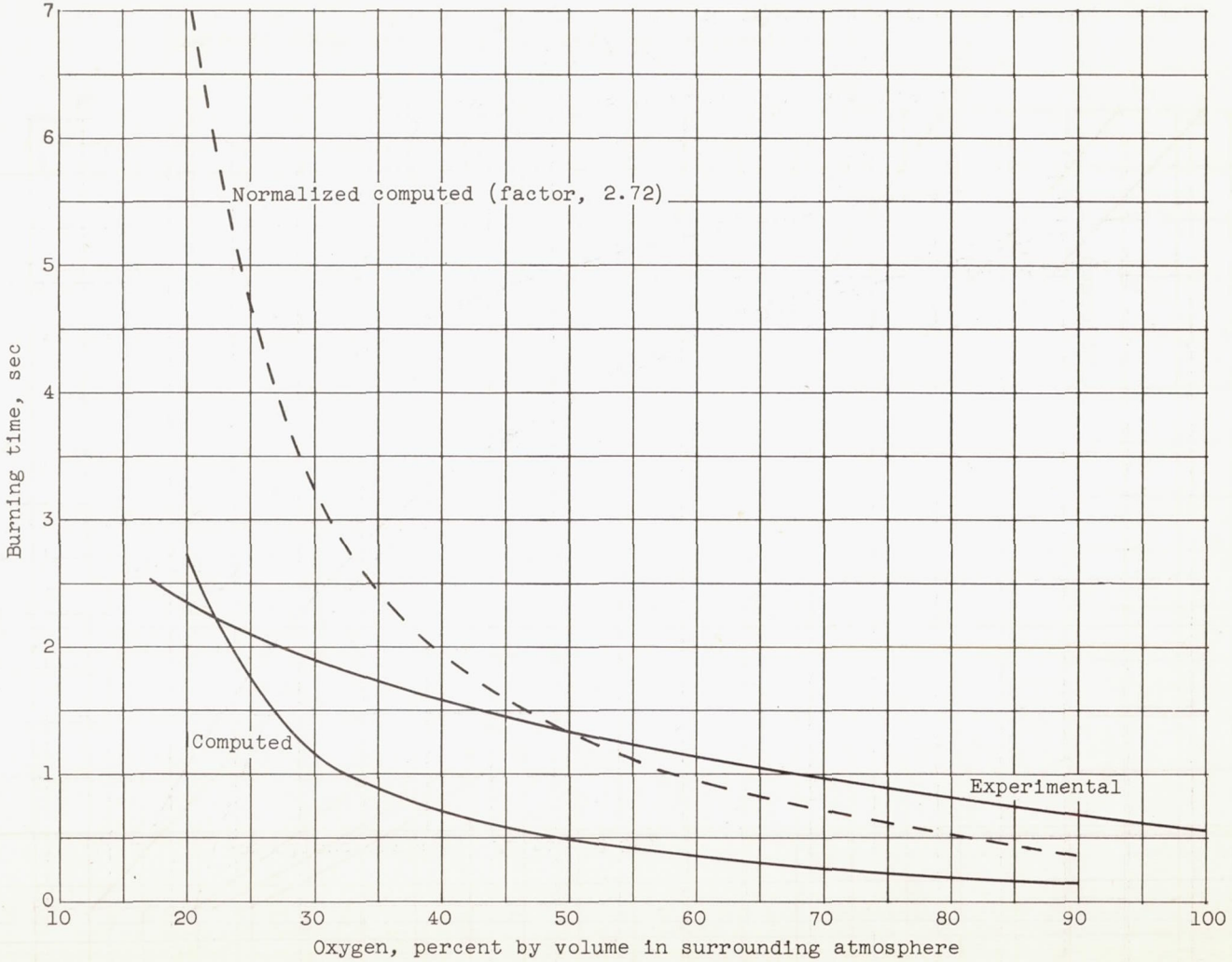

(c) Helium.

Figure 11. - Concluded. Variation of burning time with oxygen concentration and inert gases.

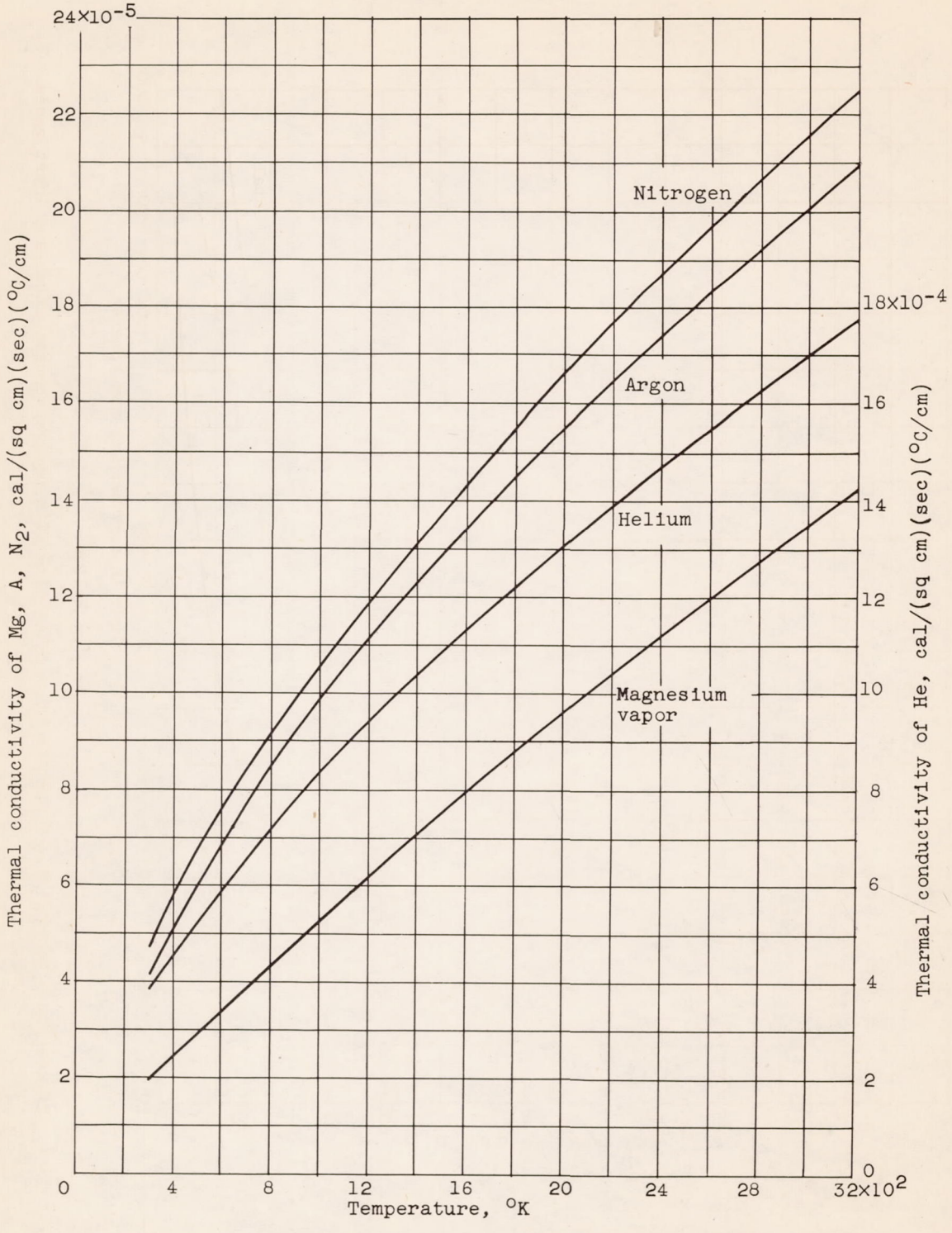

Figure 12. - Thermal conductivities used in integrations.